Contact Damage in Brittle Coating Layers: Influence of Surface Curvature

Tarek Qasim,[1] Mark B. Bush,[1] Xiaozhi Hu,[1] Brian R. Lawn[2]

[1]School of Mechanical Engineering, The University of Western Australia, Crawley, W.A. 6009, Australia

[2]Materials Science and Engineering Laboratory, National Institute of Standards and Technology, 100 Bureau Drive, Gaithersburg, Maryland 20899-8500

Received 30 July 2004; revised 1 September 2004; accepted 1 September 2004
Published online 29 December 2004 in Wiley InterScience (www.interscience.wiley.com). DOI: 10.1002/jbm.b.30188

Abstract: Fracture from indentation by a hard sphere on bilayer systems composed of curved brittle coating layers on compliant polymeric substrates is investigated, in simulation of dental crown structures. Glass plates 1 mm thick are used as representative of enamel/crown layers, and epoxy filler substrates as representative of support dentin. Specimens with curved surfaces are prepared by pressing the glass plates onto steel sphere dies with radius of curvature down to 4 mm, to reflect common occlusal geometries. The influence of curvature on the conditions to initiate and propagate subsurface "radial" cracks, widely believed to be the principal failure mode in ceramic-based dental crowns, is studied. Finite element calculations are used to evaluate stress states in the specimens. It is shown that surface curvature can play an important role in the radial crack evolution, initially by inhibiting initiation but subsequently, in the case of convex curvature, by strongly enhancing propagation to failure. Implications concerning the design of ceramic-based dental crowns are considered. © 2004 Wiley Periodicals, Inc.* J Biomed Mater Res Part B: Appl Biomater 73B: 179–185, 2005

Keywords: curved surfaces; radial cracks; contact damage; brittle layers; crown failure

INTRODUCTION

Brittle layers on compliant substrates are of high interest for their relevance to dental crowns and other biomechanical implant structures,[1–8] as well as to a variety of engineering applications including tribological and electronic packaging devices.[5] The combination of a hard, brittle outer layer and a compliant, tough inner layer offers high wear resistance and damage tolerance, factors that are crucial to the lifetime of such structures. Currently, the lifetimes of ceramic-based crowns are unacceptably short,[9–13] limited by any one of a number of damage modes that may develop in either the coating or the substrate. Of these modes, radial cracking at the coating undersurface, from flexure induced by concentrated loads at the top surface, has been identified as the most deleterious in the context of system survival.[5] These cracks are especially dangerous in thinner coatings (typically <1 mm), because they can spread long distances subsurface, in severe cases to the specimen extremities, resulting in premature failure.

Whereas many studies have been reported on damage modes in brittle/compliant bilayers of the kind under consideration here, virtually all have concentrated on flat surfaces.[2–8,14–22] Those studies have enabled determination of dependencies of critical loads for various damage modes on geometrical variables like layer thickness and indenter sphere radius, as well as on material properties like interlayer elastic modulus mismatch, brittle-layer strength, hardness, and toughness. However, teeth and crowns exhibit pronounced curvature and shape irregularities, which can substantially alter stress states and thereby influence critical loads to initiate and propagate radial cracks in the brittle layers. Controlled experiments documenting such effects need to be conducted.

Accordingly, this study aims to measure the effect of changing specimen surface curvature on the evolution of subsurface radial cracks in concentrated top-surface loading. To this end, borosilicate glass plates 1 mm thick are molded over steel sphere dies at elevated temperatures to produce hollow glass hemispheres. The hemispheres are then bonded to an epoxy resin base to produce bilayers with either convex or concave surfaces with radii of curvature down to 4 mm. A tungsten carbide sphere of radius 4 mm (representative of dental cuspal radii)[1,23] is used to apply an axisymmetric load

Correspondence to: B.R. Lawn (e-mail: brian.lawn@nist.gov)
Contract grant sponsor: the Australian Research Council
Contract grant sponsor: a Gledden Senior Fellowship at UWA
Contract grant sponsor: the U.S. National Institute of Dental and Craniofacial Research; contract grant number: PO1 DE10976

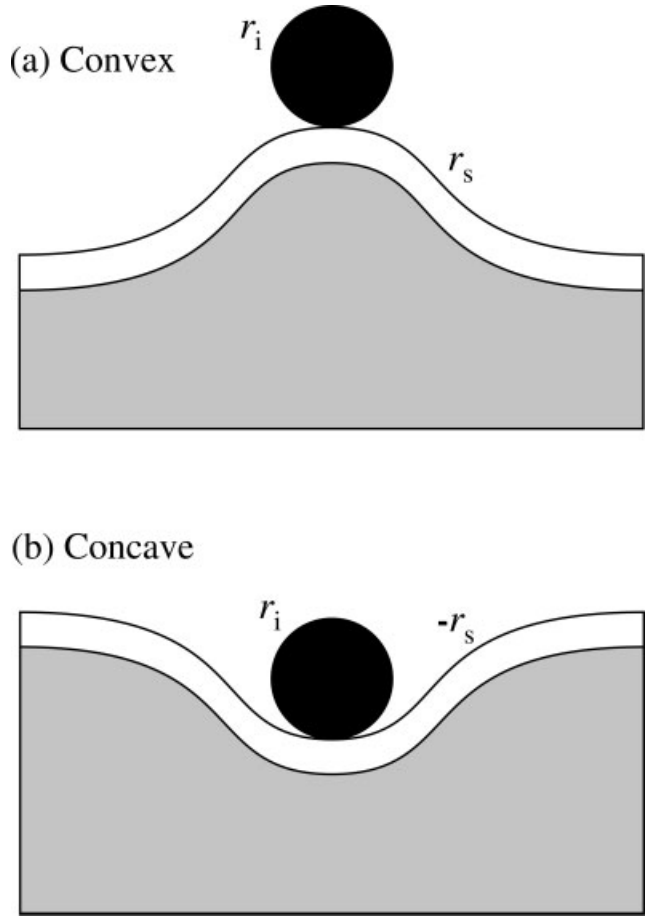

Figure 1. Loading of indenter of radius r_i on (a) convex and (b) concave curved brittle layers of inner radius r_s on compliant substrates.

on the specimen top surfaces. This choice of sphere radius is not critical, because radial cracking is insensitive to conditions at the surface contact.[24] Radial crack evolution is followed *in situ* using a video camera system. Results are interpreted using a finite element analysis (FEA) of the stress states at the brittle layer undersurfaces. It is demonstrated that increasing positive (convex) surface curvature can raise the load to initiate the first cracks, but that this same curvature can diminish the loads to ultimate failure.

EXPERIMENTAL PROCEDURE

Glass/epoxy layer structures were fabricated to model dental systems with curved surfaces, as indicated in Figure 1. Borosilicate silicate glass (D263, Menzel-Glaser, Postfach, Germany) was chosen as the brittle layer, in the form of plates $75 \times 50 \times 1$ mm. This glass has a Young's modulus of 73 GPa, close to that of dental enamel or crown porcelains. Epoxy resin (Resin R2512, ATL Composites, Southport, Australia) was chosen as the support material, because of its ease in molding to the shape of the glass overlayer and for its good bonding qualities.

To obtain curved surfaces, the glass plates were slumped over stainless steel balls of prescribed radii and subjected to a heat treatment. To prevent the glass from sticking to the steel spheres, the heated spheres were sprayed with kiln wash (50 wt % Kaolin + 50 wt % alumina hydrate, mixed with 5 parts by volume of distilled water) at ≈230°C. The sprayed film was then lightly smoothed with a lint-free cloth. The glass plates were then subjected to the following heat treatment, in air: (1) heat to ≈750°C and hold until the glass plates conform to the spherical die curvature; (2) rapid cool to solidify the plates; (3) anneal at ≈560°C and cool slowly to room temperature to avoid any residual stresses. Glass surfaces with inner radii of curvature $r_S = \infty$ (flat), 20, 15, 11, 8, and 4 mm were prepared in this way. The glass retained its original thickness of 1 mm during this treatment.

The prospective undersurfaces of the glass plates were given an abrasion treatment with 50 μm sand particles using a dental sandblast machine (P-G4000, Harnish & Rieth, Winterbach, Germany). Sandblasting is used by dental practitioners to remove excess material at the inner surfaces of crowns, as well as to enhance subsequent bonding to the residual tooth structure.[25] In our case, the treatment introduces surface flaws and thereby reduces the strength level of the glass close to that of porcelain (which fails from internal microstructural flaws). Most important, it favors preferential radial crack initiation at the glass undersurface, eliminating complications from premature cone cracking at the top surface.[6,15] Some undersurfaces were left in their as-formed state, for comparison.

The glass plates were then fitted into a mold of the same lateral dimensions, with the hemispherical protrusion facing either outward [convex surfaces, $r_S > 0$, Figure 1(a)] or inward [concave surfaces, $r_S < 0$, Figure 1(b)], and with the abraded surface always facing inward. Epoxy resin was then poured slowly into the mold to a substrate depth of about 15 mm, with intermittent vibration to remove air bubbles.

Indentation tests were carried out in air using a tungsten carbide sphere of radius $r_i = 4$ mm mounted in a screw-driven mechanical testing machine (Instron 4301, Instron Corp., Canton, MA). Care was taken to align the sphere and specimen axes so that the contact occurred axisymmetrically. Loads up to 2000 N could be attained in this configuration. During loading, the specimens were viewed from the side and slightly from above using a video camera, such that the contact and side walls of the specimens were within the field of view at all times (although not as clearly in the more concave specimens, where the sphere obstructed the surface view). A light source was placed behind the specimens to optimize crack visibility. A single-cycle axisymmetric indentation was performed on each specimen, and critical loads to initiate radial cracks at the glass undersurfaces were monitored. Subsequent propagation of the radial cracks with further increase in the loading was then followed to the point of failure (where applicable); that is, when the cracks reached the extremities of the curved surfaces. The indentation loading rate was $\approx 10\ \mathrm{N \cdot s^{-1}}$. Some 5 to 10 separate tests were run at each surface radius for the convex specimens, and three

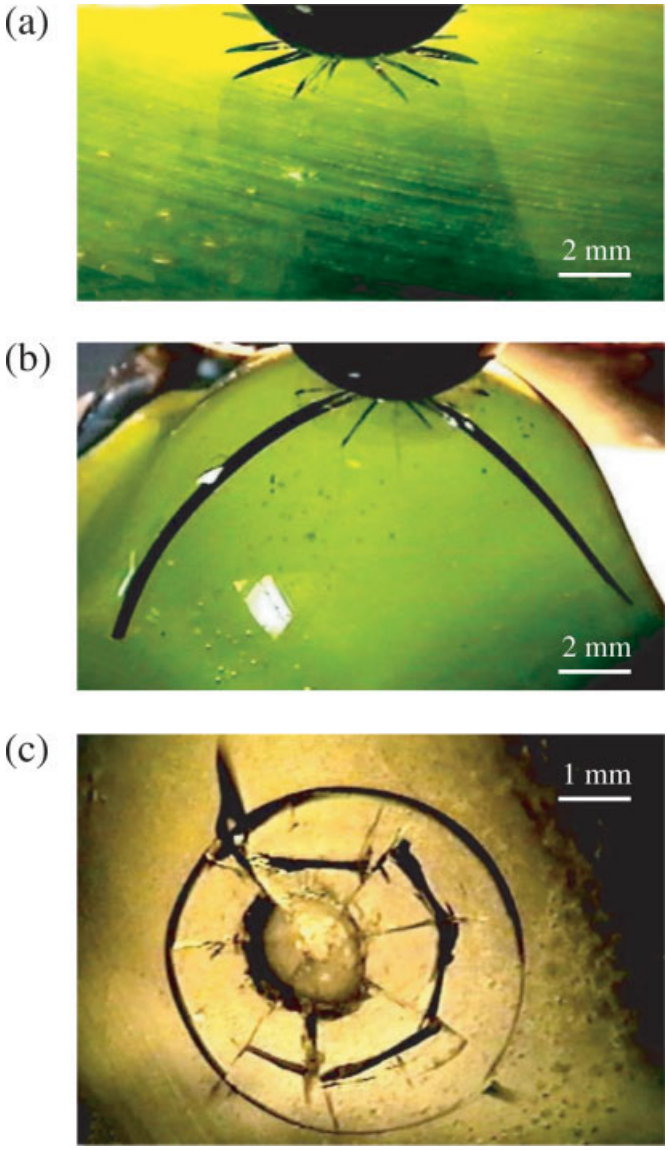

Figure 2. Radial cracks in glass layer of thickness 1 mm with abraded undersurface on epoxy resin substrate, from loading with WC sphere of radius $r_i = 4$ mm at load $P = 1500$ N: (a) flat surface, $r_S = \infty$, (b) convex surface, $r_S = 8$ mm, (c) concave surface, $r_S = -8$ mm. [Note change of scale in Figure 2(c).]

tests per surface radius for the concave specimens. No delamination was observed between the glass and epoxy in any of the tests until ultimate failure, attesting to the good bonding.

Finite element modeling was used to compute stresses in the glass layers, specifically the tensile hoop (tangential) stress at the undersurface. Algorithms for such calculations have been well documented in the literature.[2,6,19,22,26,27] Here, we used a procedure described by Ford et al.,[22] using ABAQUS software. The specimen geometries were those of Figure 1, with lateral dimensions 8 × 8 mm and thickness 6 mm + r_s. Input Young's modulus and Poisson's ratio were 73 GPa and 0.21 for the glass, 3.4 GPa and 0.33 for the epoxy, and 614 GPa and 0.3 for the tungsten carbide indenter. The meshes were systematically refined, particularly in the critical glass undersurface region, until the solutions attained convergence. Loads were applied monotonically over the experimental range from 0 to 2000 N.

RESULTS

Crack Morphology

Representative photographs from video sequences demonstrate the main effects of surface curvature on radial crack

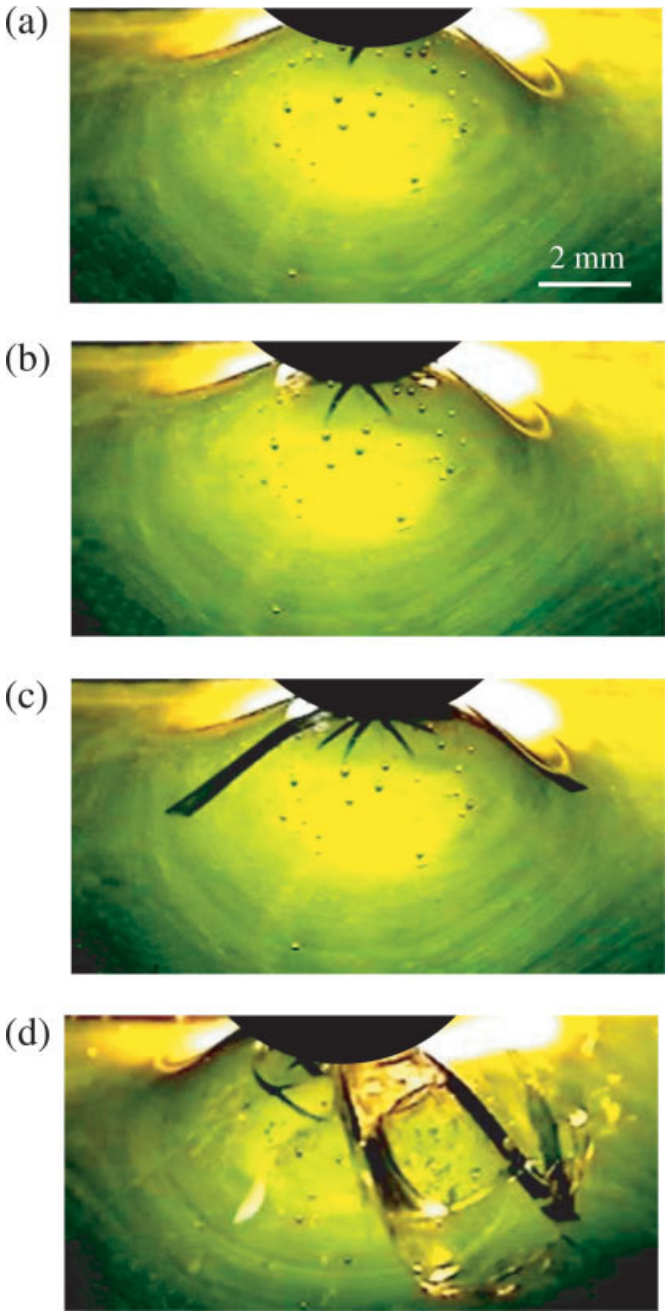

Figure 3. Video sequence showing radial crack evolution in glass layer of thickness 1 mm with abraded undersurface on epoxy resin substrate, from loading with WC sphere of radius $r_i = 4$ mm on a convex surface of radius $r_S = 4$ mm: loads (a) $P = 200$ N, (b) $P = 400$ N, (c) $P = 700$ N, (d) $P = 743$ N.

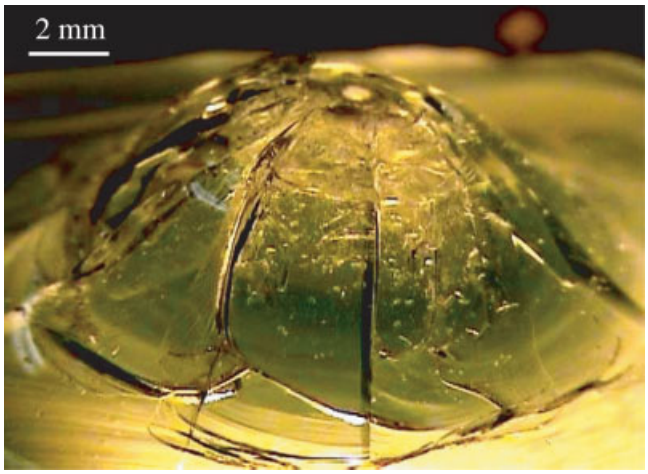

Figure 4. Complete failure of glass layer of thickness 1 mm with unabraded undersurface on epoxy resin substrate, from loading with WC sphere of radius r_i = 4 mm at load P = 710 N on a convex surface of radius r_S = 4 mm.

geometry. Figure 2 compares crack patterns in specimens with surface radius (a) $r_s = \infty$ (flat), (b) r_s = 8 mm (convex), and (c) $r_s = -8$ mm (concave), for common indentation load P = 1500 N and undersurface sandblast abrasion treatment. Figure 2(a, b) was taken *in situ*, Figure 2(c) after unloading (cracks obscured by indenter in concave specimen). An exaggerated radial crack propagation in the convex surface relative to the flat surface is clearly evident. In Figure 2(b), some radial arms have extended to the hemispherical base, whereas in Figure 2(a) they remain confined to the locality of the indenter. The latter confinement is even more evident in the concave specimens [Figure 2(c)], where the radial crack arms are to some degree encompassed by outer ring cracks at the top surface;[15] confined crack patterns of this type were evident in all concave specimens. Ring cracks were also visible at the top surface of the flat and convex surfaces after unloading, but were less restrictive, suggesting that they occurred after initiation of the radials in these overloading and undersurface-abrasion conditions.

Figure 3 shows a sequence of video clips during indentation of a convex surface with surface radius r_s = 4 mm, undersurface again abraded. Some cracks appear to initiate after others, but may still overtake their predecessors and ultimately become dominant. Notwithstanding these variations, the crack evolution pattern was relatively reproducible in the abraded specimens. Steady propagation of the radial cracks from the near-contact zone to the base of the hemispherical surface and through the thickness of the glass layer was a consistent feature of convex specimens. At higher loads, the radial cracks linked up at their base, causing separation and dislodgement of triangular glass segments [Figure 3(d)]. Top surface ring cracks were apparent in the unloaded specimens, but again were preceded by the radials.

More variability was observed in the crack patterns for unabraded glass surfaces, especially in the initial stages. Generally, higher loads were required to form the cracks, and the ensuing pop-in was more abrupt. The radial crack densities also tended to be lower than in the unabraded surfaces, and the preferential extension of some arms relative to their neighbors more erratic. At higher loads, however, the radials extended steadily, as in abraded surfaces. In some highly convex specimens, the initiation load was so high that the radial cracks popped-in without interruption to the base, resulting in instantaneous failure, as in Figure 4.

Quantitative Radial Crack Evolution

Critical loads P_R to initiate subsurface radial cracks in the curved glass surfaces were measured as a function of specimen curvature r_s^{-1}. Data are plotted in Figure 5 for abraded and unabraded specimens and for convex and concave surfaces, as means and standard deviation bounds. Solid lines are from FEA computations, using best-fit strengths S = 75 MPa for abraded surfaces and S = 295 MPa for unabraded glass (typical values for abraded and as-polished glass surfaces[15]) to determine critical loads. The computations do not pass through all the data, especially for unabraded surfaces, but do at least account for the principal data trends. Interestingly, the FEA critical load function passes through a minimum a little below $r_s^{-1} = 0$, approaching a factor of 2 increase at the extremities of the curvature range covered.

Figure 6 shows typical plots of circumferential radial crack length s (i.e., crack length measured around the curved undersurface) as a function of indenter load, for abraded convex specimens of specified radius r_s. The data for the flat surface were truncated at the maximum available load 2000 N. Analogous data for concave surfaces could not be obtained as easily because of obstruction by the indenter, but those available from postmortem examinations [e.g., Figure 2(c)] indicate slight shifts to the left of the $r_s = 0$ curve. In the convex surfaces, the popped-in radial cracks first extend

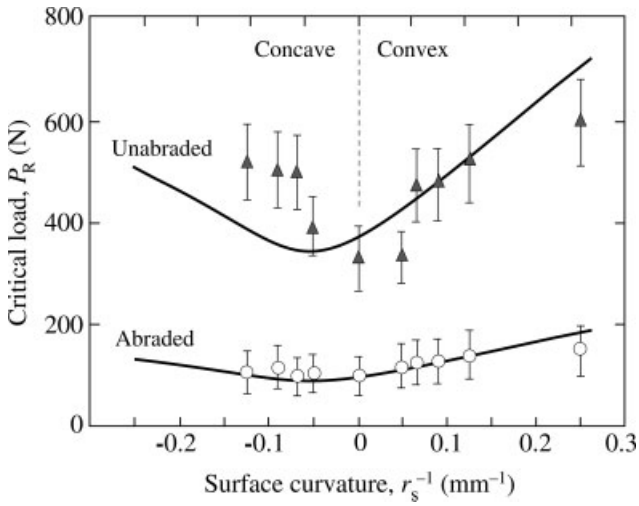

Figure 5. Critical load P_R to initiate radial cracks in glass layer of thickness 1 mm with abraded glass undersurfaces, as function of glass surface curvature r_S^{-1}. Loading with WC sphere of radius r_i = 4 mm. Data shown for abraded and unabraded surfaces, means and standard deviations. Solid lines are FEA computations.

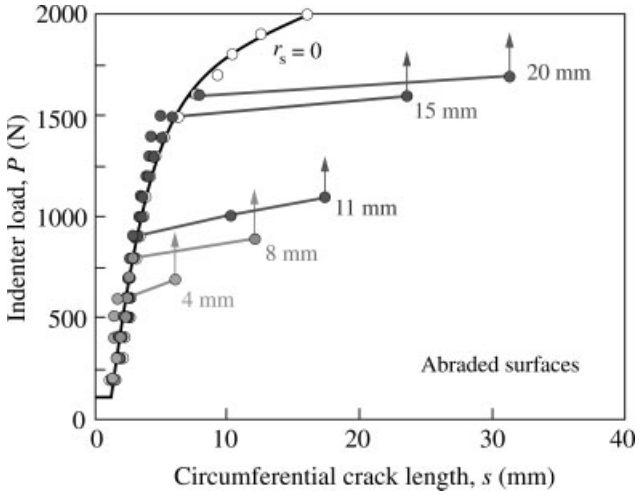

Figure 6. Evolution of radial cracks in convex glass surfaces of specified radius r_S and thickness 1 mm with abraded undersurfaces, from monotonic loading with WC sphere of radius $r_i = 4$ mm. Note abrupt propagation to edge of glass base. Arrows indicate further loading on arrested cracks. Tests for flat surface truncated at $P = 2000$ N.

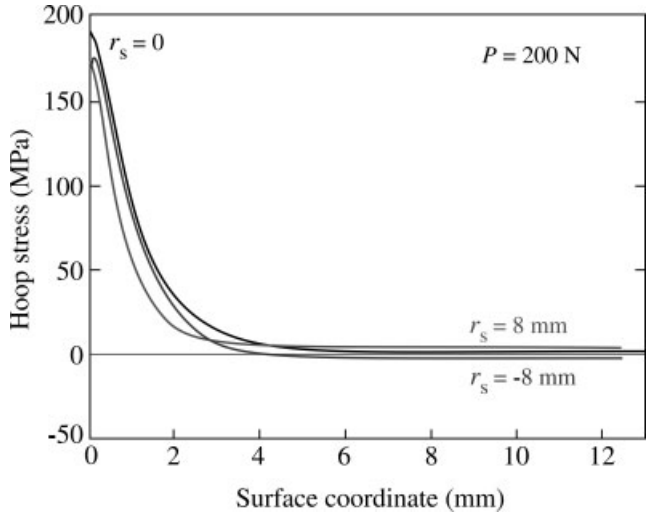

Figure 8. Plot of hoop tensile stress (stress normal to plane of diagram) at undersurface of glass layer on epoxy substrate as a function of circumferential coordinate, WC sphere load $P = 200$ N. Curves shown for glass radius $r_S = 8$ mm (convex), $r_S = \infty$ (flat) and $r_S = -8$ mm (concave). Note crossover of curves.

steadily with increasing load [e.g., Figure 3(a, b)], but then propagate relatively abruptly to the base of the hemispherical cap [Figure 3(c)], with increasing abruptness at smaller r_s. Still further increase in load does not extend the cracks onto the surrounding flat surface of the glass plate but instead causes linkage of neighboring radial arms and, ultimately, material dislodgement [Figure 3(d)]. This final stage in the failure process is indicated in Figure 6 by vertical arrows. The loads to achieve crack propagation to the base [i.e., Figure 3(c)] are summarized in Figure 7 over all such tests, for both abraded and unabraded specimens. Whereas the effect of surface curvature on this "failure" condition is strongly evident in Figure 7, that of the surface flaw state is not as pronounced.

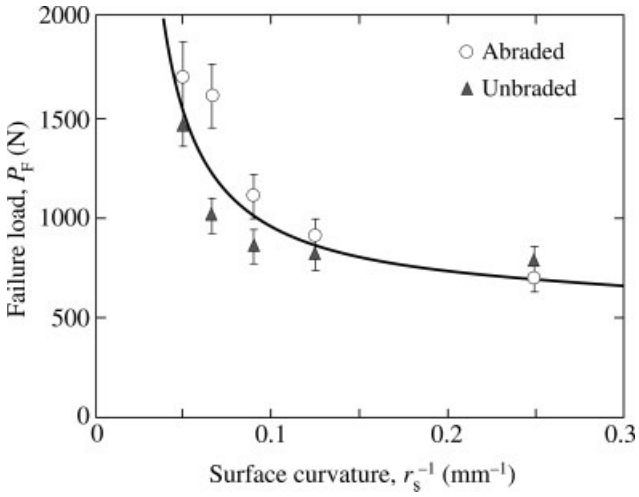

Figure 7. Failure loads to propagate radial cracks to base of convex glass layers of radius r_S and thickness 1 mm with abraded undersurfaces, from loading with WC sphere of radius $r_i = 4$ mm. Data shown for abraded and unabraded surfaces, means and standard deviations. Solid curve is empirical spline fit. Tests for flat and concave surfaces truncated at $P = 2000$ N.

An attempt at a theoretical analysis of the propagation characteristics for popped-in radial cracks has previously been made for flat surfaces, taking into account the effect of stress gradients at the coating undersurface on the stress–intensity factor.[27] Extension of such analysis to curved surfaces lies beyond the scope of the present study. Nevertheless, simple FEA computations shed some insight into the influence of surface curvature. Figure 8 plots the radial distribution of hoop tensile stress at the glass undersurface for representative convex ($r_s = 8$ mm), flat ($r_s = \infty$) and concave ($r_s = -8$ mm) layers at a common indentation load ($P = 200$ N). Note that some of the curves in the plot cross each other. The tensile stresses along the contact axis are maximum in the flat layers, accounting for the relatively low critical loads for radial crack initiation in Figure 5. At the same time, the range of these tensile stresses is longer in the convex layers and shorter in the concave layers, enhancing the later stages of crack propagation in the former case but confining them in the latter.

DISCUSSION

We have investigated the initiation and propagation of radial cracks in curved brittle coating layers on compliant substrates from axisymmetric contacts at the top surface. The results highlight the importance of surface curvature in the fracture behavior. Generally, it requires higher contact loads to initiate radial cracks in curved surfaces (Figure 5), most notably in convex but also in concave surfaces—the curvature diminishes the undersurface tensile stress immediately below the

contact (Figure 8). It follows that widely practiced tests on model flat-layer surfaces[5,6] provide useful conservative estimates for first radial cracking in more convoluted geometries. The influence of curvature is felt more strongly in the propagation stages of radial fracture in convex surfaces, not so much immediately after pop-in but in a more profound manner as the cracks extend around the circumference, where the cracks abruptly accelerate toward the hemispherical base (Figure 6). The reason for the accelerated failure is to be found in the greater spatial range of tensile stresses in the more positively curved surfaces (Figure 8). Hence the failure load, here defined as that required to propagate radial cracks to the support base, diminishes systematically with increasing convexity (Figure 7). Further increased loading ultimately causes the radial cracks to link at the base, dislodging material segments [Figures 3(d) and 4].

The results in this study are highly relevant to the failure of ceramic-based dental crowns. As mentioned, radial cracking is widely believed to be a principal mode of crown failure.[10,23] Convex surfaces would seem to be especially vulnerable to sudden crack propagation through the entirety of the crown. The crown must then be replaced[11]—prolonged oral function can only lead to severe fragmentation. The clear message is to avoid sharp convex curvatures in the crown construction. Use of the present data to make *quantitative* predictions of failure are more ambitious, for several reasons: we have used epoxy resin as the outerlayer support, which is considerably less stiff than dentin; tooth geometry is more convoluted than the simple curved surfaces used herein; our experiments have used only 1 mm layer thicknesses—thinner layers will diminish the loads required to initiate and propagate the radial cracks;[6,24] real crowns are not "built-in" to a flat surround layer, but are cemented at their margins to the tooth structure; we have considered only single-cycle loading—slow crack growth and fatigue in the repeat loading that characterizes oral function must exacerbate the failure process, and may even introduce new modes of failure, especially in aqueous environments.[21,28,29] Nevertheless, the methodology does provide useful guidelines for data trends.

The results for concave surfaces pertain to the failure of ceramic acetabular cup liners for total hip replacements.[4,5,30] Again, tests on flat layers may be used to provide a conservative baseline for estimating failure loads. In this case, the fractures are more likely to remain localized around the contact site rather than propagate to the edges of the device. However, once damage is initiated, continued articulating contact with a ceramic ball joint can only exacerbate wear and lead to more severe damage, in which case the critical load for radial crack initiation may be considered to define an effective failure condition.

An issue that requires attention is that of flaw state. Radial crack initiation at the brittle undersurface is determined when the tensile stress exceeds the strength (at least to first approximation).[27] The sandblast treatment used in our experiments to reduce strength variability of the glass plates diminishes the critical load for first fracture by introducing larger surface flaws (Figure 5).[25] However, this may not be a major factor in the porcelains and other polycrystalline ceramic materials used in real crowns, because those materials already contain a profusion of internal microstructural flaws. In any case, once the radial crack has popped in and begins its propagation, it is the intrinsic material toughness that governs the mechanics, and flaw state becomes a much less important factor in the ultimate failure condition (Figure 8).

The authors gratefully acknowledge useful discussions with Chris Ford, Matthew Rudas, Yu Zhang, and Do Kyung Kim. Information of product names and suppliers in this artricle is not to imply endorsement by NIST.

REFERENCES

1. Peterson IM, Pajares A, Lawn BR, Thompson VP, Rekow ED. Mechanical characterization of dental ceramics using hertzian contacts. J Dent Res 1998;77:589–602.
2. Jung YG, Wuttiphan S, Peterson IM, Lawn BR. Damage modes in dental layer structures. J Dent Res 1999;78:887–897.
3. Lawn BR, Lee KS, Chai H, Pajares A, Kim DK, Wuttiphan S, Peterson IM, Hu X. Damage-resistant brittle coatings. Adv Eng Mater 2000;2:745–748.
4. Lawn BR. Ceramic-based layer structures for biomechanical applications. Curr Opin Solid State Mater Sci 2002;6:229–235.
5. Lawn BR, Deng Y, Miranda P, Pajares A, Chai H, Kim DK. Overview: Damage in brittle layer structures from concentrated loads. J Mater Res 2002;17:3019–3036.
6. Deng Y, Lawn BR, Lloyd IK. Characterization of damage modes in dental ceramic bilayer structures. J Biomed Mater Res 2002;63B:137–145.
7. Shrotriya P, Wang R, Katsube N, Seghi R, Soboyejo WO. Contact damage in model dental multilayers: An investigation of the influence of indenter size. J Mater Sci Mater Med 2003; 14:17–26.
8. Lawn BR, Pajares A, Zhang Y, Deng Y, Polack M, Lloyd IK, et al. Materials design in the performance of all-ceramic crowns. Biomaterials 2004;25:2885–2892.
9. Kelly JR. Ceramics in restorative and prosthetic dentistry. Annu Rev Mater Sci 1997;27:443–468.
10. Kelly JR. Clinically relevant approach to failure testing of all-ceramic restorations. J Prosthet Dent 1999;81:652–661.
11. Malament KA, Socransky SS. Survival of dicor glass-ceramic dental restorations over 14 years: I. Survival of dicor complete coverage restorations and effect of internal surface acid etching, tooth position, gender and age. J Prosthet Dent 1999;81:23–32.
12. Malament KA, Socransky SS. Survival of dicor glass-ceramic dental restorations over 14 years: II. Effect of thickness of dicor material and design of tooth preparation. J Prosthet Dent 1999; 81:662–667.
13. Malament KA, Socransky SS. Survival of dicor glass-ceramic dental restorations over 16 years: Part III: Effect of luting agent and tooth or tooth-substitute core structure. J Prosthet Dent 2001;86:511–519.
14. Wuttiphan S. Contact damage and fracture of ceramic layer structures. PhD thesis Dissertation, University of Maryland, 1997.
15. Chai H, Lawn BR, Wuttiphan S. Fracture modes in brittle coatings with large interlayer modulus mismatch. J Mater Res 1999;14:3805–3817.
16. Zhao H, Hu XZ, Bush MB, Lawn BR. Contact damage in porcelain/Pd-alloy bilayers. J Mater Res 2000;15:676–682.
17. Zhao H, Hu X, Bush MB, Lawn BR. Cracking of porcelain coatings bonded to metal substrates of different modulus and hardness. J Mater Res 2001;16:1471–1478.

18. Lee C-S, Lawn BR, Kim DK. Effect of tangential loading on critical conditions for radial cracking in brittle coatings. J Am Ceram Soc 2001;84:2719–2721.
19. Miranda P, Pajares A, Guiberteau F, Cumbrera FL, Lawn BR. Contact fracture of brittle bilayer coatings on soft substrates. J Mater Res 2001;16:115–126.
20. Zhao H, Miranda P, Lawn BR, Hu X. Cracking in ceramic/metal/polymer trilayer systems. J Mater Res 2002;17:1102–1111.
21. Lee C-S, Kim DK, Sanchez J, Miranda P, Pajares A, Lawn BR. Rate effects in critical loads for radial cracking in ceramic coatings. J Am Ceram Soc 2002;85:2019–2024.
22. Ford C, Bush MB, Hu XZ, Zhao H. A Numerical study of fracture modes in contact damage in porcelain/Pd-alloy bilayers. Mater Sci Eng 2004;A364:202–206.
23. Lawn BR, Deng Y, Thompson VP. Use of contact testing in the characterization and design of all-ceramic crown-like layer structures: A review. J Prosthet Dent 2001;86:495–510.
24. Rhee Y-W, Kim H-W, Deng Y, Lawn BR. Contact-induced damage in ceramic coatings on compliant substrates: fracture mechanics and design. J Am Ceram Soc 2001;84:1066–1072.
25. Zhang Y, Lawn BR, Rekow ED, Thompson VP. Effect of sandblasting on the long-term strength of dental ceramics. J Biomed Mater Res 2004;71B:381–386.
26. Fischer-Cripps AC, Lawn BR, Pajares A, Wei L. Stress analysis of elastic–plastic contact damage in ceramic coatings on metal substrates. J Am Ceram Soc 1996;79:2619–2625.
27. Kim H-W, Deng Y, Miranda P, Pajares A, Kim DK, Kim H-E, et al. Effect of flaw state on the strength of brittle coatings on soft substrates. J Am Ceram Soc 2001;84:2377–2384.
28. Zhang Y, Lawn BR. Long-term strength of ceramics for biomedical applications. J Biomed Mater Res 2004;69B:166–172.
29. Zhang Y, Pajares A, Lawn BR. Fatigue and damage tolerance of Y-TZP ceramics in layered biomechanical systems. J Biomed Mater Res 2004;71B:166–171.
30. Willmann G. Ceramic femoral heads for total hip arthroplasty. Adv Eng Mater 2000;2:114–122.